

# Comparison of thermal neutron detection efficiency of ${}^6\text{Li}$ scintillation glass and ${}^3\text{He}$ gas proportional tube\*

XU Ming(徐明)<sup>1,2</sup> TANG Zhi-Cheng(唐志成)<sup>1:1)</sup> CHEN Guo-Ming(陈国明)<sup>1</sup> TAO Jun-Quan(陶军全)<sup>1</sup>

<sup>1</sup> Institute of High Energy Physics, Chinese Academy of Sciences, Beijing 100049, China

<sup>2</sup> University of Chinese Academy of Sciences, Beijing 100049, China

**Abstract:** We report on a comparison study of the  ${}^3\text{He}$  gas proportional tube and the  ${}^6\text{Li}$  incorporated scintillation glasses on thermal neutron detection efficiency. Both  ${}^3\text{He}$  and  ${}^6\text{Li}$  are used commonly for thermal neutron detection because of their high neutron capture absorption coefficient. By using a neutron source  ${}^{252}\text{Cf}$  and a paraffin moderator in an alignment system, we can get a small beam of thermal neutrons. A flash ADC is used to measure the thermal neutron spectrum of each detector, and the detected number of events is determined from the spectrum, then we can calculate the detection efficiency of different detectors. Meanwhile, the experiment has been modeled with GEANT4 to validate the results against the Monte Carlo simulation.

**Key words:** thermal neutron, detection efficiency,  ${}^6\text{Li}$  incorporated scintillation glass,  ${}^3\text{He}$  gas proportional tube, flash ADC, GEANT4

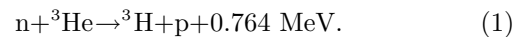
**PACS:** 28.20.Fc, 24.10.Lx **DOI:** 10.1088/1674-1137/37/10/106001

## 1 Introduction

Space activities have been increased considerably in the past decades [1]. Electron/hadron discrimination power is an important factor for space experiments designed to study cosmic rays at high energy. Electromagnetic calorimeters have good intrinsic electron/hadron rejection power based on the shower topology, and this property requires the calorimeters with high granularity read out and sufficient depth so that the showers can fully develop. Unfortunately, in space experiments, due to power consumption limitations and weight constraints, the electron/hadron discrimination capability is reduced. The number of secondary neutrons in the hadronic shower is much larger than that in the electromagnetic shower, therefore to place a neutron detector downstream of the calorimeter, aimed to exploit the neutron components of the shower, is a feasible solution to enhance the electron/hadron discrimination capability. Neutrons produced in the shower are with typical kinetic energies of a few MeV [2]. Generally, there are two kinds of method for the neutron detection. One is the fast neutron detection with elastic scattering, in which neutrons lose their kinetic energy at their initiated energies. The other is thermal neutron detection, neutrons captured by the nucleus after they have lost practically all their kinetic energy through the thermalization process. Fast

neutron detection requires low background environment, because the ionization signal generated from elastic scattering is small. Considering the neutron detector is to be put downstream of the electromagnetic calorimeter, a large number of charged particle can be produced in the shower as the background to neutron detector. Therefore it is difficult to pick up the neutron signal from such a background. The thermal neutron detection is based on nuclear reactions. As the signal generated from neutron absorption is much larger than the ionization signal of the charged particles, it is a more appropriate solution.

Many types of thermal neutron detector have been developed, like the gas filled tube, liquid organic scintillator and solid state scintillator [3, 4]. Thermal neutron detection is based on nuclear reactions. Because of their high neutron capture absorption coefficient, both isotopes of  ${}^3\text{He}$  and  ${}^6\text{Li}$  are used commonly for detecting thermal neutrons.  ${}^3\text{He}$  gas proportional tube is a typical thermal neutron detector, the reaction when a neutron is absorbed by  ${}^3\text{He}$  is:



The reaction produces a triton and a proton, which are emitted in opposite directions and cause ionizations in the tube. The pulse from the proportional tube is fed into a preamplifier, which enlarges the signal for the following up device to record. Lithium glass is a scintilla-

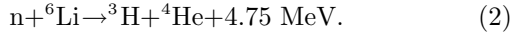
Received 5 December 2012, Revised 18 March 2013

\* Supported by National Natural Science Foundation of China (11061140514)

1) E-mail: tangzhch@mail.ihep.ac.cn

©2013 Chinese Physical Society and the Institute of High Energy Physics of the Chinese Academy of Sciences and the Institute of Modern Physics of the Chinese Academy of Sciences and IOP Publishing Ltd

tion type detector, for neutron detection, often enriched with the isotope  ${}^6\text{Li}$ , the nuclear reaction of  ${}^6\text{Li}$  by capturing a thermal neutron, releasing a triton and an alpha particle:



Lithium glass thus emits light in response to excitation energy received from ionizing radiation, and the output is usually collected by a photomultiplier.

GEANT4 is a widely used toolkit for the simulation of the passage of particles through matter [5]. Its fields of application include high energy, nuclear and accelerator physics, as well as studies in medical and space science. As such, it can handle many physically possible processes, including decay, nuclear interaction and particle production. GEANT4 includes facilities for handling geometry, tracking, detector response, run management, visualization and user interface, the detector response is recording when a particle passes through the volume of the detector, and uses a suitable physics list approximating how a real detector would respond. For many physics processes, this means less time need be spent on the low level details, and a user can start immediately on the more important aspects of the simulation. The geometry of the efficiency measurement experiment has been accurately modeled with GEANT4, including the physical layout, detectors, and the materials.

## 2 Experiment and Simulation Setup

### 2.1 Experiment

The  ${}^3\text{He}$  tube used in this experiment is made by GE. It has a 1 inch inner diameter and 1 meter length, with filled pressure 10 atm including 80%  ${}^3\text{He}$  gas and 20% Isobutane gas, and 304 stainless steel as the outer shell. A cadmium coat is covered from both ends of the tube as the thermal neutron absorber, only a length of 8 cm in the middle of the tube left, exposed as the sensitive area.

The lithium glasses are of type ST-602, made by CNNC Beijing Nuclear Instrument Factory. There are three round pieces with thickness 1 mm, 2 mm and 3 mm, the diameter of these glasses are 2 cm.

As the two kinds of detector have different geometries, the best solution for detection efficiency comparison is to use a small area of thermal neutron beam. In this experiment, by assembling a neutron source  ${}^{252}\text{Cf}$  and a paraffin moderator in an alignment system made of a paraffin barrel, which is covered with thermal neutron absorber, we can get the thermal neutron flow from this system. The radius of the paraffin barrel is 29 cm, with the inner 24 cm part made by paraffin and the outer 5 cm part made by boron-containing paraffin; the height of the barrel is 60 cm. In the middle of the barrel, a

collimation hole with dimension of 2 cm radius and 20 cm height is scooped, where the  ${}^{252}\text{Cf}$  source and a 5 cm long paraffin moderator are placed. There are 20 layers of 1 mm thickness boron-containing plastic, each layer with 1 cm radius hole in the center, placed on the top of the paraffin barrel as the thermal neutron absorber and alignment.

${}^3\text{He}$  tube and lithium glasses are put on the top center of the paraffin barrel separately for each measurement. In the case of  ${}^3\text{He}$ , a pair of preamplifiers are connected to both ends of the detector, because the magnification factor of the detector itself is very weak. After the preamplifier, a fan in/out module is used to add the signal from both ends of the detector, and the output is copied to two channels, one for trigger, another for spectrum measurement. For lithium glasses measurement, the setup is almost the same as the  ${}^3\text{He}$  tube, only except for without the preamplifier, because a photon multiplier tube is applied as the lithium glass readout, and this kind of detector has sufficient magnification factor. Finally, a Flash ADC is used to record the pulse shape of each event.

For each kind of detector, two sets of measurement are implemented for 120 minutes. Firstly, the apertural boron-containing plastic is placed at the center of the barrel, with positional relationship shown in the left plot of Fig. 1, both signal from the collimation hole and the background are collected. Then this boron-containing plastic is replaced with another set of complete plastic plates of the same thickness, as shown in the right plot of Fig. 1, which fully covers the top of the paraffin barrel. The positional relationship of the detectors and the paraffin barrel is unchanged. In this case, only the background is collected. The only difference between these two measurements is the thermal neutron flux from the central hole. Therefore, the difference of these two measurements represents the contribution from the center collimation hole of the plastic plates, and it makes a thermal neutron beam-like source with this kind of setup.

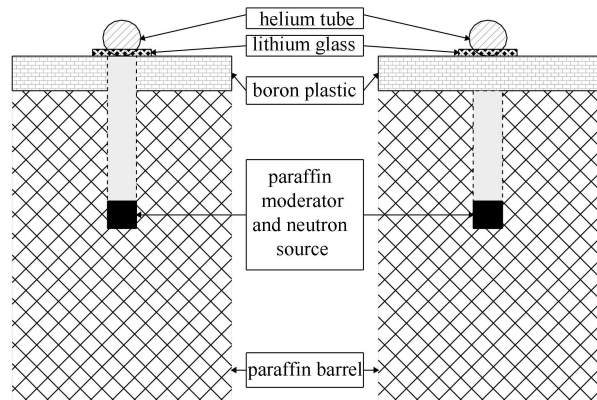


Fig. 1. Schematic diagram of the experiment setup.

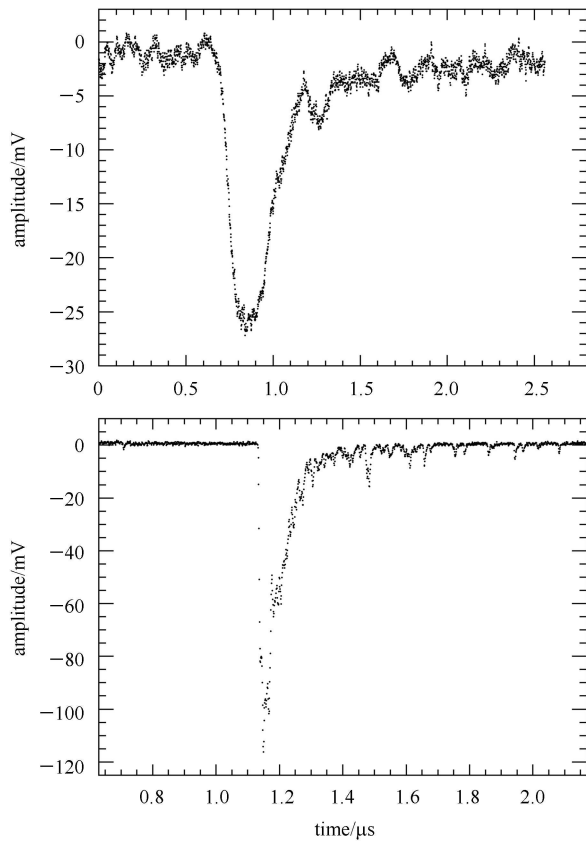


Fig. 2. Upper one and lower one respectively represent  $^3\text{He}$  tube pulse shape and 1 mm  $^6\text{Li}$  glass pulse shape recorded by flash ADC.

## 2.2 Monte Carlo simulation

The experiment setup has been accurately modeled with GEANT4 to validate the results with the Monte Carlo simulation. The same experimental geometry and materials used in the measurement were modeled within GEANT4. A complete list of materials used is given in Table 1.

Experiment comparison with GEANT4 simulations are done at the level of the energy deposition in lithium glasses and  $^3\text{He}$  tube, without modeling of readout chain response in the simulation. GEANT4 provides a user-customizable physics list that may be changed to suit the requirement of the simulation. The simulated samples have been produced using a physics list suitable for the case [6]: QGSP\_BIC\_HP, with Binary Cascade model and Quark-Gluon String Precompound model to generate the final state for hadron inelastic scattering respectively below 10 GeV, with addition to use the data driven high precision neutron package to transport neutrons below 20 MeV down to thermal energies. With the same setup as in the measurement, a typical size of 1 million events with isotropic emission of  $4\pi$  solid angle is generated each time. The emission spectrum of the neutron source as shown in Table 2.

Table 1. A description of the composition of materials in the simulation.

| material          | $\rho/(\text{g}/\text{cm}^3)$ | element | $A/(\text{g}/\text{mol})$ | fraction(mass) |
|-------------------|-------------------------------|---------|---------------------------|----------------|
| paraffin          | 0.93                          | H       | 1.01                      | 0.15           |
|                   |                               | C       | 12.01                     | 0.85           |
| boron pastic      | 1.03                          | H       | 1.01                      | 0.08           |
|                   |                               | C       | 12.01                     | 0.87           |
|                   |                               | B       | 10.81                     | 0.05           |
| lithium glass     | 2.8                           | O       | 16.00                     | 0.44           |
|                   |                               | Na      | 22.99                     | 0.09           |
|                   |                               | Si      | 28.09                     | 0.32           |
|                   |                               | Ca      | 40.08                     | 0.11           |
|                   |                               | Li      | 6.90                      | 0.35           |
|                   |                               | Li      | 7.98                      | 0.05           |
| $^3\text{He}$ gas | 0.0089                        | He      | 3.00                      | 1              |
| isobutane gas     | 0.005                         | H       | 1.01                      | 0.17           |
|                   |                               | C       | 12.01                     | 0.83           |
| steel             | 7.5                           | Fe      | 55.85                     | 1              |

Table 2. MC neutron emission spectrum.

| energy/MeV | relative intensity |
|------------|--------------------|
| 0.1        | 0.06               |
| 0.5        | 0.45               |
| 1.0        | 0.90               |
| 2.0        | 1.0                |
| 3.0        | 0.84               |
| 4.0        | 0.63               |
| 5.0        | 0.41               |
| 6.0        | 0.24               |
| 7.0        | 0.13               |
| 8.0        | 0.09               |
| 9.0        | 0.96               |
| 10.0       | 0.92               |

## 3 Results and discussion

### 3.1 Event number counting

By integrating the pulse recorded from the flash ADC Fig. 2, we can get the spectrum. With the spectrum calculated from the left case minus the right case of Fig. 1, we can get the signal from only the collimation hole. In the  $^3\text{He}$  tube case, because the neutron pulse shape is much wider than the background pulse shape, only the signal with pulse width greater than 200 ns is integrated for the spectrum, the detected number of events can be calculated by adding the counts of the subtraction spectrum Fig. 3. Lithium glasses suffer from the photomultiplier noise and other radiation, so using Gaussian function to fit the subtraction spectrums is a solution, as shown in Fig. 4, and the number of events under the fitted Gaussian function is the detected number of events from the collimation hole.

The efficiency of the detector is defined as the ratio of the number of detected neutron-induced interactions divided by the number of incident neutrons. In this

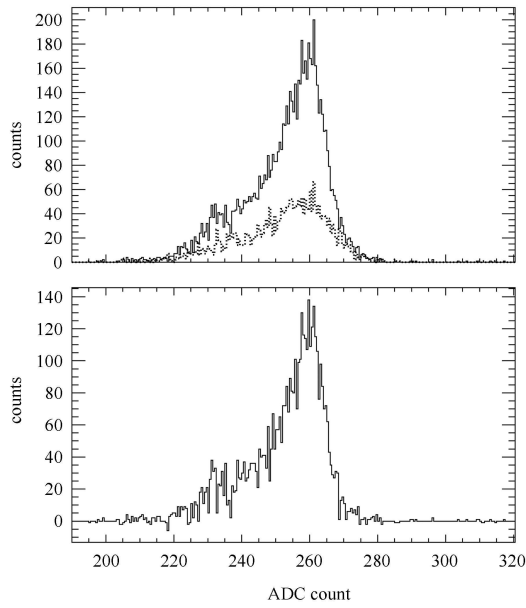


Fig. 3. Neutron spectrum in the experiment obtained by using  $^3\text{He}$  tube. Solid and dashed line are respectively the spectrum of  $^3\text{He}$  tube in the left case and right case of Fig. 1, the lower plot is the solid line minus the dashed of the upper plot, which means the spectrum of thermal neutron only from the collimation hole.

paper, we determine the number of detected thermal neutrons from the measured spectrums, and calculate the number of incident thermal neutrons by fitting of detection efficiency versus different detector thickness of lithium glasses with experiment data. The half life of  $^{252}\text{Cf}$  is about 2.6 years, so we can assume radioactive source strength is unchanged in all measurements. For the Lithium glasses of different thickness, there is a relationship between the detection efficiency and detector thickness [7]:

$$\eta(d) = 1 - (1 - \eta_1)^d, \quad (3)$$

$$N_{\text{det}}(d) = N_0 [1 - (1 - \eta_1)^d], \quad (4)$$

$\eta(d)$  stands for the efficiency of lithium glass with thickness  $d$ ,  $N_{\text{det}}$  and  $N_0$  regard to neutron-induced events and incident neutron events respectively. For the absolute efficiency,  $N_0$  can be determined by the fitting of the function with the experiment data of different thickness lithium glass scintillator.

### 3.2 Systematic error estimation

The diameters of the collimator hole and the  $^3\text{He}$  tube are 2 cm and 2.5 cm respectively, which means that the geometry relationship of the collimator hole and the

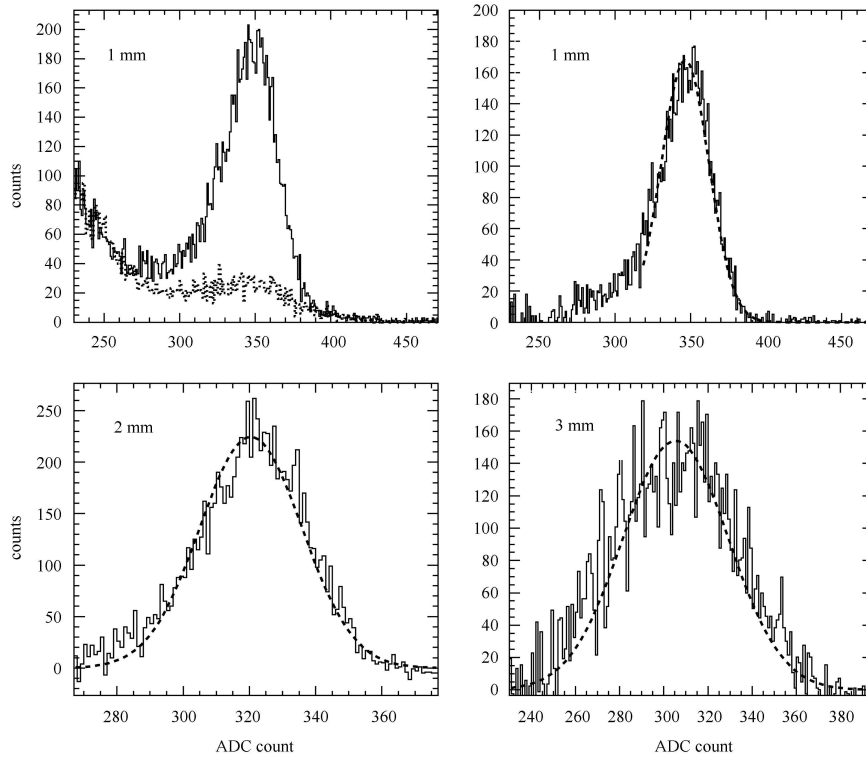


Fig. 4. Neutron spectrum in experiment obtained by using lithium glasses. Solid and dashed line in the upper left plot are respectively the spectrum of 1 mm lithium glass in the left case and right case of Fig. 1. The remaining three plots are the subtraction spectrums of 1 mm, 2 mm and 3 mm lithium glass, the dashed lines are the Gaussian fitting functions; the number of events under the fitted Gaussian function represents the number of thermal neutron events from the collimation hole.

barrel is the most sensitive factor to the systematic error. The  $^3\text{He}$  tube is measured several rounds, and using the standard deviation of the measurements as the event number uncertainty:

$$\Delta N_{^3\text{He}} = \sqrt{\frac{\sum_i^n (N_i - \bar{N})^2}{n}}. \quad (5)$$

When the area of lithium glasses is much larger than the collimator hole, the spatial relationship will not introduce much systematic error. The detected thermal neutron number of lithium glasses are determined by the fitting of the measured spectrums as shown in Fig. 4. That means the uncertainty of fitting is the most sensitive factor to the systematic error and the fitting error can be treated as the event number uncertainty  $\Delta N_{6\text{Li}}$ .

The total incident number of events  $N_0$  and event number uncertainty  $\Delta N_0$  can be determined by the fitting of formula 4 with the experiment data of lithium glasses. The detection efficiency is the ratio of detected number of events divided by the number of incident number of events:

$$\epsilon_{\text{det}} = \frac{N_{\text{det}}}{N_0}, \quad (6)$$

and the uncertainty on the efficiency  $\epsilon_{\text{det}}$  is<sup>1)</sup>:

$$\Delta \epsilon_{\text{det}} = \frac{1}{N_0} \sqrt{(1-2\epsilon_{\text{det}})(\Delta N_{\text{det}})^2 + \epsilon_{\text{det}}^2 (\Delta N_0)^2}. \quad (7)$$

The systematic error of the detection efficiency  $\Delta \epsilon_{\text{det}}$  is shown in Table 3.

Table 3. Number of events and detection efficiency.

| detector           | $N_{\text{det}}$ | $\epsilon_{\text{det}}(\%)$ | $\epsilon_{\text{det}}(\text{MC})(\%)$ |
|--------------------|------------------|-----------------------------|--|
| 1 mm               | 6096±323         | 61.4±4.0                    | 59.3                                   |
| 2 mm               | 8694±477         | 87.5±4.6                    | 85.4                                   |
| 3 mm               | 9257±491         | 93.2±4.6                    | 92.9                                   |
| $^3\text{He}$ tube | 6777±407         | 68.2±4.1                    | 70.5                                   |

## 4 Conclusion

We try to find a neutron detector with sufficient detection efficiency which is designed to enhance electromagnetic calorimeters in electron/hadron discrimination. Both lithium glasses and  $^3\text{He}$  tube have been tested with neutron source, and data compared with an accurate GEANT4 simulation. The 1 mm thickness lithium glass has a thermal neutron detection efficiency of about 60% Fig. 5, almost the same as the  $^3\text{He}$  tube within

the error range. The efficiency increases as the detector thickness, and can reach 90% by using the 3 mm

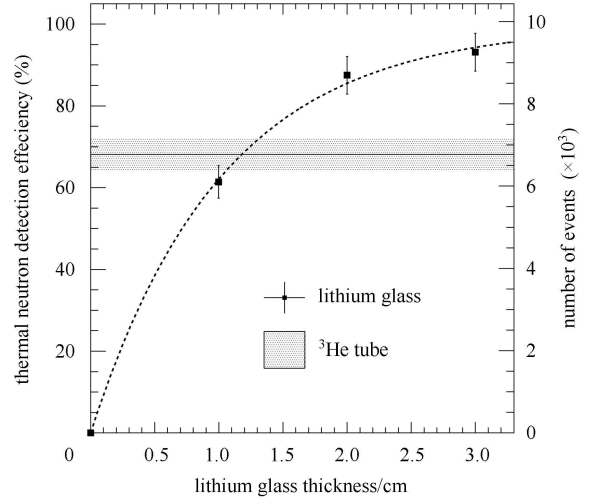


Fig. 5. Thermal neutron detection efficiency and number of events of 1 mm, 2 mm, 3 mm lithium glass and  $^3\text{He}$  tube in the measurement using formula 4 to fit the event number of different thickness lithium glass  $N_{\text{det}}(d)$  to get the total incident thermal neutron events  $N_0 = 9937 \pm 698$ ; the dashed line is the theoretical relationship between detection efficiency and detector thickness.

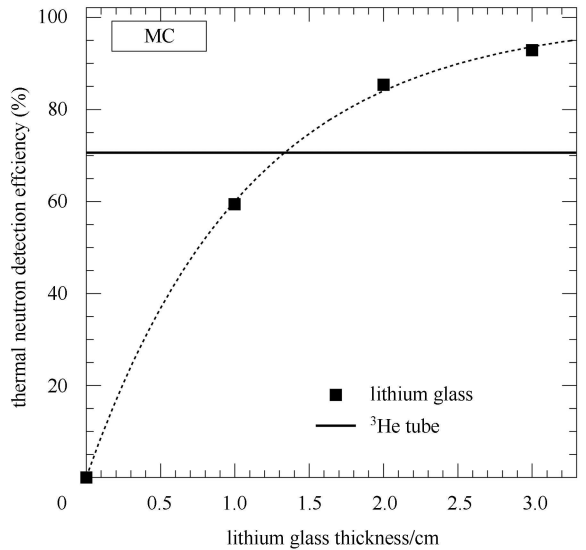


Fig. 6. Monte Carlo simulation on thermal neutron detection efficiency and number of events of 1 mm, 2 mm, 3 mm lithium glass and  $^3\text{He}$  tube.

1) since  $N_{\text{det}}$  is a subset of  $N_0$ , the correlation between  $N_{\text{det}}$  and  $N_0$  is  $N_{\text{det}}$ , the covariance matrix of  $(N_{\text{det}}, N_0)$  will be in the form of  $\text{cov}(N_{\text{det}}, N_{\text{det}}) = (\Delta N_{\text{det}})^2$ ,  $\text{cov}(N_0, N_0) = (\Delta N_0)^2$ ,  $\text{cov}(N_{\text{det}}, N_0) = \text{cov}(N_0, N_{\text{det}}) = (\Delta N_{\text{det}})^2$ , with the derivative  $\frac{\partial \epsilon_{\text{det}}}{\partial N_0} = \frac{-\epsilon_{\text{det}}}{N_0}$ ,  $\frac{\partial \epsilon_{\text{det}}}{\partial N_{\text{det}}} = \frac{1}{N_0}$ , and  $(\Delta \epsilon_{\text{det}})^2 = \text{cov}^2(\epsilon_{\text{det}}) = [(1-2\epsilon_{\text{det}})(\Delta N_{\text{det}})^2 + \epsilon_{\text{det}}^2 (\Delta N_0)^2] / N_0^2$  [8].

thickness lithium glass. Results demonstrate in general good agreement between data and simulation Fig. 6. The choice of detector for a particular application is determined by the experiment's requirements with respect to additional detector characteristics, such as required size, sensitivity to background radiation such as gamma-rays, counting rate capability, and position stability as a

function of time. To choose a suitable thermal neutron detector in space experiments, these factors should all be considered in further studies.

*We would like to thank Dr. Sun Zhi-Jia of China Spallation Neutron Source IHEP team for his suggestions and assisting us in using the  $^3\text{He}$  tube.*

---

## References

- 1 Cervelli F. Nuclear Instruments and Methods in Physics Research A, 2004, **535**: 25–35
- 2 Gabriel T A, Groom D E, Job P K, Mokhov N V, Stevenson G R. Nuclear Instruments and Methods in Physics Research A, 1994, **338**: 336–347
- 3 Peurrung A J. Nuclear Instruments and Methods in Physics Research A, 2000, **443**: 400–415
- 4 Knoll G F. Radiation Detection and Measurement. 4rd edition. Chapter 14-15. New Jersey: John Wiley and Sons Ltd, 2010
- 5 Agostinelli S et al. Nuclear Instruments and Methods in Physics Research A, 2003, **506**: 250–303
- 6 Geant4 physics reference manual. [http://geant4.cern.ch/support/proc\\_mod\\_catalog/physics\\_lists/referencePL.shtml](http://geant4.cern.ch/support/proc_mod_catalog/physics_lists/referencePL.shtml)
- 7 McGregor D S, Hammig M D, YANG Y H, Gersch H K, Klann R T. Nuclear Instruments and Methods in Physics Research A, 2003, **500**: 272–308
- 8 James F E. Statistical Methods in Experimental Physics. 2nd edition. Chapter 8.5.2. Singapore: World Scientific Publishing Co. Pte. Ltd., 2006